Chinese Science Bulletin

Microscopic study on stress-strain relation of granular materials

LIU SiHong[1†], YAO YangPing[2], SUN QiCheng[3], LI TieJun[1] & LIU MinZhi[1]

[1] State Key Laboratory of Hydrology-Water Resources and Hydraulic Engineering, Hohai University, Nanjing 210098, China;
[2] Department of Civil Engineering, Beihang University, Beijing 100191, China;
[3] State Key Laboratory of Hydroscience and Engineering, Tsinghua University, Beijing 100084, China

A biaxial shearing test on granular materials is numerically simulated by distinct element method (DEM). The evolution of the microstructures of granular materials during isotropic compression and shearing is investigated, on which a yield function is derived. The new yield function has a similar form as the one used in the modified Cam-clay model and explains the yield characteristics of granular materials under the isotropic compression and shear process through the change of the contact distribution $N(\theta)$ defining the contacts at particle contact angle θ.

DEM, granular materials, yield surface, microstructure

Granular materials, like sands, consist of particles and surrounding voids. The macro-mechanical behavior of granular materials is therefore inherently related not only to the distinct particles constituted, but also to its inner microstructures reflecting how distinct particles are arranged in space. In the past decades, great efforts have been devoted to study the macroscopic mechanics behavior of granular materials in terms of its microstructures. For example, Oda[1] studied the particle contact normals of sand samples after triaxial compression tests, and found that the frequency distribution of particle contact normals concentrates on the direction of the major principle stress during shearing. Matsuoka[2] carried out direct shear tests on assemblies of both photoelastic and aluminum rods, on which a stress-shear dilatancy equation was derived from the frequency distribution of particle contacts on the mobilized plane. Wang et al.[3] studied the development of the stress self-organizing process during the outbreak of slope debris flows and the critical properties of the clayey debris transmission, so as to reveal the mechanism of the debris flows and forecast debris flows. On the hypothesis of the unsaturated soil mechanics and the theory of multiphase porous media, Zhao and Zhang[4] gave an expression for the total deformation work and proposed a formula of the effective stress in unsaturated soil. Zhen and Jin[5] established a material model for particulate materials to characterize the cyclical distribution of the elastic modulus and the thermal expansion coefficient in space, by taking the thermal stress distribution and the particle interaction into account.

Experiments and theoretical analysis have been two main approaches for studying the mechanical behaviors of granular materials in early times. As granular materials consist of particles, it is more realistic to study their mechanical behaviors if we use distinct element approaches in which the particle arrangement is modeled explicitly. Recent distinct element approaches started with the distinct element method (DEM) that was first developed by Cundall (1971) for rock mass problems and later applied to granular materials by Cundall and Strack[6]. DEM can provide sufficient model micromechanical data such as the displacement of individual particles, contact orientations, contact forces and mobilized

Received June 16, 2009; accepted August 13, 2009
doi: 10.1007/s11434-009-0599-z
†Corresponding author (email: sihongliu@hhu.edu.cn)
Supported by the National Natural Science Foundation of China (Grant Nos. 10672050, 10872016)

Citation: Liu S H, Yao Y P, Sun Q C, et al. Microscopic study on stress-strain relation of granular materials. Chinese Sci Bull, 2009, 54: 4349−4357, doi: 10.1007/s11434-009-0599-z

inter-particle frictional angles. It is based on the Newton's Second Law of Motion, and does not need constitutive models as used in continuum approaches, which are gotten from experiments or experiences. Thus, DEM is especially fit for studying the mechanism of granular materials. For example, it has been applied to studying the stress-dilatancy relation[7,8], wetting-induced collapse mechanism[9,10] and slope failure mechanism[11,12] of granular soils. The commercial DEM code of PFC2D has been applied to simulating the forming and developing of shear band in sandy soil, and studying the mechanism of seepage by Zhou et al.[13,14].

In this article, a biaxial shearing test of granular media is numerically simulated by DEM. The evolution of the microstructures, defining the distribution of the inter-particle contacts with respect to contact angles, during isotropic compression and shearing, is investigated, and the explanation for it is made as well. The relation between the macroscopic stress-strain variables and microscopic variables on the mobilized plane are discussed. Based on the evolution of the microstructures, a yield function for granular materials is derived, which has a similar form as the one in the modified Cam-clay model.

1 Discrete modeling of biaxial shearing test

The distinct element method (DEM), which models materials as packed assemblies of discrete elements, enables us to analyze the micromechanics of granular materials. Although the method can treat any shape of element, all the granular elements in this study are treated as disks. Each disk is assumed to be a rigid body, but the disks can slightly overlap with each other at their contact points. Further, relative movements between neighboring disks which give rise to separation or slippage are allowed during calculations. Figure 1 shows the contact model for rigid disks. It consists of two parts: (1) a stiffness model providing a linear elastic relation between contact force and contact relative displacement in normal and shear directions; and (2) a slip model enforcing a relation of Coulomb's type between shear and normal contact forces[6]. Due to the dynamic formation of the model, energy dissipation through frictional sliding may not be sufficient to reach a steady-state solution. Additional dissipation is achieved by small amount of viscous damping. As shown in Figure 1, the granular materials parameters used in DEM numerical analysis

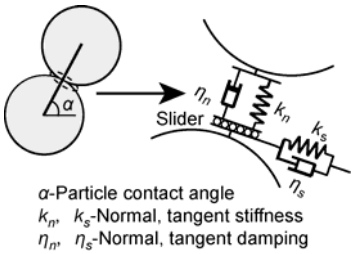

Figure 1 DEM particle contact model.

include the normal and tangent stiffness (k_n, k_s), damping ratio (η_n, η_s) and inter-particle friction angle ϕ_μ.

In this work, we simulate a biaxial shearing test using DEM. The DEM specimen consists of 5651 circular particles (disks) 5 mm and 9 mm in diameter (mixing ratio of 3:2 by area), which is generated randomly within a 53 cm by 36 cm rectangular area that is bounded by four rigid walls. The specimen has an initial void ratio of 0.2685. The input parameters used in our simulation are summarized in Table 1, which correspond to the properties of aluminum material. The stiffness (k_n, k_s) is obtained from the contact theory[15] of two elastic discs by considering the stress level possibly applied on the granular sample; the damping ratio (η_n, η_s) is the critical attenuation coefficient of the single degree-of-freedom system vibration, i.e. $2\sqrt{km}$. The inter-particle friction angle $\phi_\mu = 16°$ is obtained from the frictional tests on aluminum rods. The time step Δt is chosen to be 1/10 times the critical time step Δt_c in order to maintain a quasi-static state during the calculation, where $\Delta t_c = 2\sqrt{m/k}$ is based on the single degree-of-freedom system of a mass m connected to ground by a spring of stiffness k. In the past, the parameters in Table 1 were used in simulating direct shear, simple shear and biaxial compression tests on assemblies of aluminum rods with diameters of 5 mm and 9 mm and a mixing ratio of 3:2 by weight. The simulation results agreed very well with the experimental results[7–10,16,17]. By the way, aluminum rods can ideally simulate granular materials in a two-dimensional manner, as the specific gravity of aluminum rods is 2.69, close to that of real soil particles (about 2.65), and the assembly of aluminum rods can stand without any additional support on the front/back sides on which no frictional resistances are produced. When used in experiments, aluminum rods should be longer than 5 cm so that they can be packed. As the length of aluminum rods used is much greater than their diameter, the assembly of aluminum rods is similar to a

Table 1 Input parameters in DEM simulation

Normal stiffness k_N	Tangent stiffness k_s	Normal damping η_n	Tangent damping η_s	Inter-particle friction angle ϕ_μ	Particle density ρ
9.0×10^9 N/m^2	3.0×10^8 N/m^2	7.9×10^4 N·s/m^2	1.4×10^4 N·s/m^2	16°	2700 kg/m^3

part of strip foundations. Hence, the biaxial shearing test on the assembly of aluminum rods may be regarded as a test in plane strain state.

The DEM simulation of biaxial shearing test was performed by giving symmetrical movements to two pairs of boundary walls in horizontal and vertical directions. The walls were allowed to move only in their normal directions, but they expanded or contracted according to the principal strains of the whole area. The loading process includes isotropic (hydrostatic) compression (i.e. increasing the confining pressure p under the condition of $\sigma_1=\sigma_3$.) and shearing under the condition of a constant p (i.e. the increase of σ_1 is equal to the decrease of σ_3, so as to keep p=constant and increase the ratio of σ_1/σ_3). Figure 2 shows the e-lg$p$ curve obtained from the DEM simulation during the isotropic compression when p increases from 5 kPa to 1 MPa. Figure 3 shows the relations among the principle stress ratio σ_1/σ_3, the principle strains (ε_1,ε_3) and the volumetric strain ε_v, which are obtained from the DEM simulation during shearing under the condition of p=50 kPa. For the biaxial shearing test, $p=(\sigma_1+\sigma_3)/2$ and $\varepsilon_v=\varepsilon_1+\varepsilon_3$. It is seen from Figure 2 that although the void ratio of the DEM sample slightly changes with the increase in the confining pressure p, the simulated e-lg$p$ curve is similar to that of sands and a yielding-like stress of about 200 kPa exists during isotropic compression. During shearing, the DEM sample has such a typical behavior of granular materials as getting contracted first and then becoming dilative. The maximum ratio of the principal stresses $R=\sigma_1/\sigma_3$ is approximately 2.2, corresponding

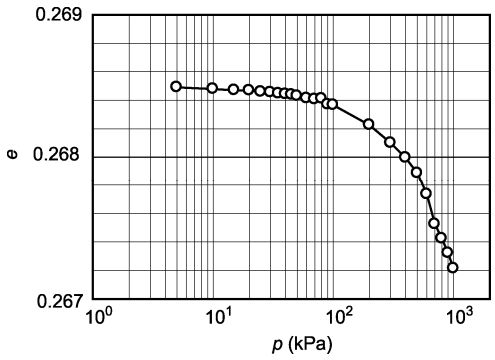

Figure 2 Numerically simulated e-lg$p$ curve during isotropic compression.

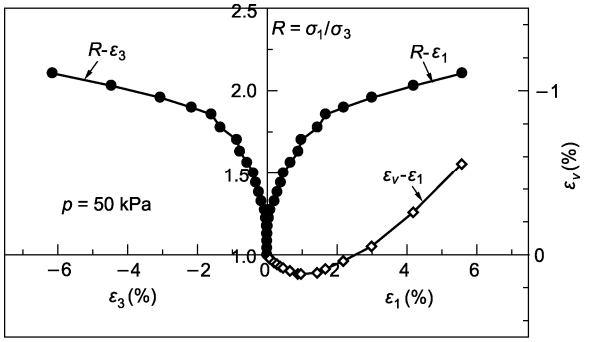

Figure 3 Numerically simulated stress-strain relation during shearing at p=50 kPa.

to an internal friction angle $\phi=22°$.

2 Changes of granular microstructures during isotropic compression and shearing

At present, there are several ways to characterize the microstructures of granular materials, such as fabric tensor[18], coordination number, comprehensive structure potential[19] and particle contact angles. In this work, the distribution of statistical particle contact points in terms of contact angles, briefly called as the distribution of particle contacts, is used. The particle contact angle is defined to be an angle of the connection line of the two contacting circular particles' centers which are inclined to a certain base level. Figure 4 illustrates two particle contact angles used in this article according to the base level: (1) the angle α. The base level is chosen to be the major principal stress σ_1 plane (horizontal plane). It is positive while counterclockwise; (2) the angle θ. The base level is chosen to be the normal of the potential mobilized plane. The potential mobilized plane corresponds to the plane on which the shear-normal stress ratio becomes a maximum, and is inclined at an angle of $45°+\phi_{mo}/2$ to the major principal stress plane. Here, ϕ_{mo} is the mobilized internal friction angle defined by $\sin\phi_{mo}=(\sigma_1-\sigma_3)/(\sigma_1+\sigma_3)$[20,21].

Figure 5 shows the distributions of particle contact forces under isotropic compression and shearing, respectively, in which the thickness of lines represents the magnitude of the contact forces. It is seen that there are

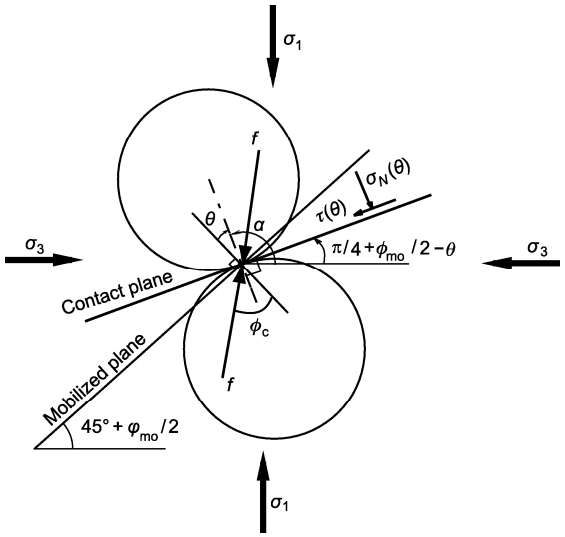

Figure 4 Definition of particle contact angles.

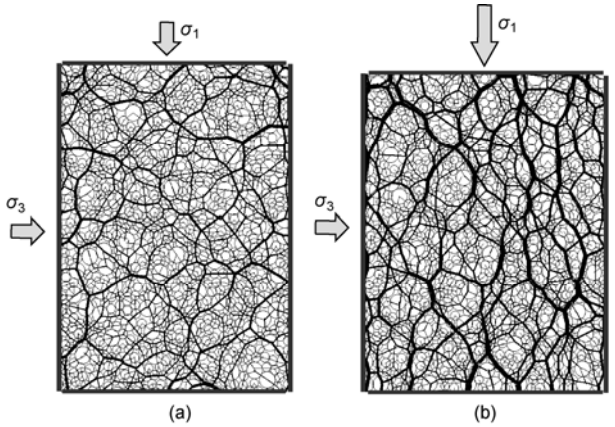

Figure 5 Distribution of particle contact forces. (a) Isotropic compression (σ_1=σ_3); (b) shear state (σ_1>σ_3).

several force chains formed by the particle contact forces, which may reflect the granular materials' microstructures. The force chains are nearly round under isotropic compression, and tend to be elliptic when the particle contact forces begin to concentrate along the direction of the major principal stress during shearing. As the particle contact forces transfer through the contacting points, the concentration of the particle contact forces along the direction of the major principal stress means the increase in the number of the particle contact points along the major principal stress. Denoting $N(\alpha)$ the number of particle contact points at the particle contact angle α (*cf.* Figure 4), the distribution of $N(\alpha)$ in accordance with Figure 5 is shown in Figure 6. It is seen that the jagged distribution of $N(\alpha)$ can be fitted by a dashed circle during isotropic compression, and it gradually changes to be peanuts-like or elliptic during shearing, which means that the anisotropy of the microstructures of the sample develops. This is one of the most typical characteristics of granular materials, which may be closely related to the mechanical behaviors of granular materials.

During shearing, there are three types of particle contact points[2,20,21]: (1) steady contact points for the particles always keeping in contact; (2) appearing contacts, for such particles that are not contacted originally but begin to contact each other; and (3) disappearing contacts, for such particles that are contacted originally but begin to separate each other. Correspondingly, there are three types of distribution functions: $N_s(\alpha)$ for the numbers of steady contact points, $N_g(\alpha)$ for the numbers of appearing contact points and $N_d(\alpha)$ for the numbers of disappearing contact points. Up to the peak strength, these three distribution functions of the simulated sample in accordance with Figure 6 are shown in Figure 7. It is seen that during shear, most particle contact points are the steady contact points $N_s(\alpha)$, the appearing contact points $N_g(\alpha)$ are close to the direction of the major principal stress σ_1 and the disappearing contact points $N_d(\alpha)$ are close to the direction of the minor principal stress σ_3. These results are similar to the ones observed by Oda et al. in physical experiments[22].

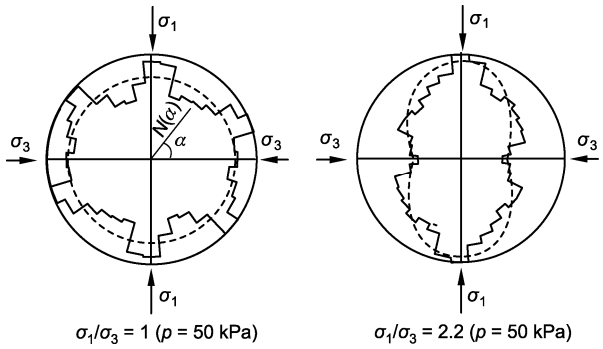

Figure 6 Distribution of particle contact points statistically counted with respect to contact angles α.

During shearing, the change of granular material microstructures is not only due to the generation of new contact points along the major principal stress σ_1 and the disappearance of contact points along the minor principal stress σ_3, but also due to the sliding and rotation of the steady contact points, which make the particle contact angles change. Let $\Delta\alpha$ be the mean change of contact angles of steady contact points for a given interval (10°) which occurs from the initial hydrostatic state to the peak stress state. $\Delta\alpha$ is taken as positive when the

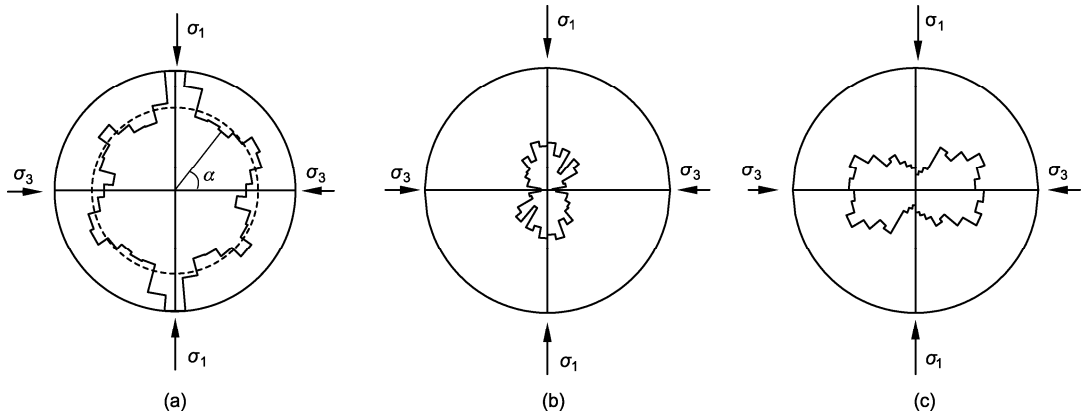

Figure 7 Distribution of the change of the contact points from the start of shear to the peak stress at p=50 kPa. (a) For steady contact points; (b) for appearing contact points; (c) for disappearing contact points.

contact angle α increases counterclockwise. The rose diagram in Figure 8 shows the mean change of the steady contact points corresponding to Figure 7(a) as a function of α. The dotted line in the same figure is fitted using the macroscopic shear-normal stress ratio, τ/σ_N, acting on a tangent plane at contact angle α. As the inclination of the tangent plane at contact angle α to the major principal stress plane is $\alpha+\pi/2$, the stress ratio τ/σ_N on the tangent plane is obtained from the Mohr's stress circle as follows:

$$\frac{\tau}{\sigma_N}=\frac{(\sigma_1-\sigma_3)\sin\{2(\alpha+\pi/2)\}}{(\sigma_1+\sigma_3)+(\sigma_1-\sigma_3)\cos\{2(\alpha+\pi/2)\}}. \quad (1)$$

From Figure 8, it can be said that the mean change of contact angles $\Delta\alpha$ is proportional to τ/σ_N, and becomes a maximum when the contact plane is parallel to a mobilized plane. This means that the relative movement at the steady contact points is primarily related to the macroscopic shear-normal stress ratio, and also seems to support the idea that the movement of particles is activated along the mobilized plane[2]. The numbers of the appearing and disappearing contact points in accordance with Figure 7(b) and (c) which count along the mobilized plane are given as a function of θ in Figure 9. The particle contact angle θ, defined on the mobilized plane (*cf*. Figure 4), varies from –90° to +90°. It is seen from Figure 9 that most of the contact points are generated on the positive side of θ, i.e. the directions effective for providing high shear resistance along the mobilized plane. However, the contacts whose contact angles θ are negative disappear.

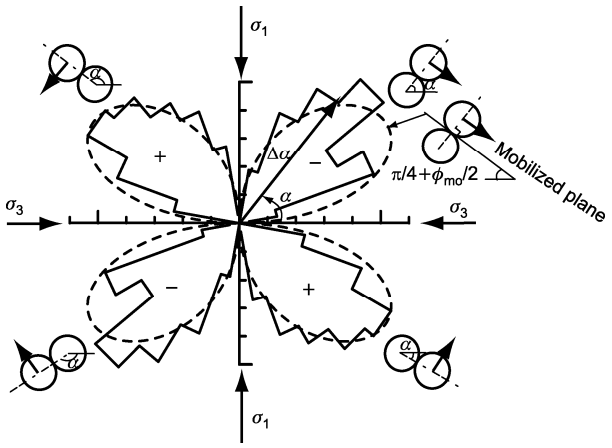

Figure 8 Distribution of mean change of contact angles $\Delta\alpha$.

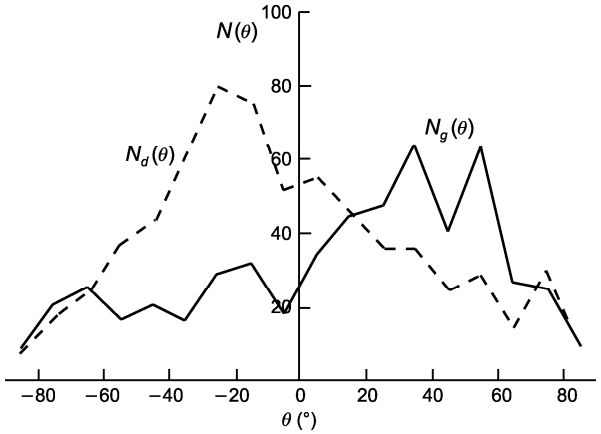

Figure 9 Distribution of appearing and disappearing particle contacts on mobilized planes.

3 Relations between macroscopic stress-strains and microstructures on mobilized plane

From the simple and direct shear tests on aluminum rods and their numerical simulations using DEM, Liu et al.[7,8] obtained the following relationships between the ma-

croscopic stress-strains of granular materials with the microstructures on the mobilized plane:

$$\frac{\tau}{\sigma_N}=\tan 3\overline{\varphi_c}-\frac{6\overline{\varphi_c}}{\pi\cos 3\overline{\varphi_c}}\cong\tan 1.08\overline{\varphi_c}, \tag{2}$$

$$-\frac{\mathrm{d}\varepsilon_N}{\mathrm{d}\gamma}=\tan 3\bar{\theta}-\frac{6\bar{\theta}}{\pi\cos 3\bar{\theta}}\cong\tan 1.08\bar{\theta}, \tag{3}$$

where $\overline{\phi_c}$ is the average inclination angle of the particle contact forces weighted by the magnitudes of the contact forces on the mobilized plane, $\bar{\theta}$ the average particle contact angles on the mobilized plane, as shown in Figure 4.

For biaxial shearing test, the stress ratio on the mobilized plane is

$$\frac{\tau}{\sigma_N}=\frac{(\sigma_1-\sigma_3)\sin\{2(\pi/4+\varphi_{\mathrm{mo}}/2)\}}{(\sigma_1+\sigma_3)+(\sigma_1-\sigma_3)\cos\{2(\pi/4+\varphi_{\mathrm{mo}}/2)\}}. \tag{4}$$

Assuming that the directions of the principal stresses are identical with those of the principal strain increments, the principal strain that increases on the mobilize plane can be calculated as

$$\left.\begin{aligned}\mathrm{d}\varepsilon_N&=\frac{\mathrm{d}\varepsilon_1-\mathrm{d}\varepsilon_3}{2}+\frac{\mathrm{d}\varepsilon_1+\mathrm{d}\varepsilon_3}{2}\cos\left\{2\left(\frac{\pi}{4}+\frac{\varphi_{\mathrm{mo}}}{2}\right)\right\},\\ \frac{\mathrm{d}\gamma}{2}&=\frac{\mathrm{d}\varepsilon_1-\mathrm{d}\varepsilon_3}{2}\sin\left\{2\left(\frac{\pi}{4}+\frac{\varphi_{\mathrm{mo}}}{2}\right)\right\},\end{aligned}\right\} \tag{5}$$

in which the mobilized internal friction angle is defined by $\phi_{\mathrm{mo}}=\tan^{-1}((\sqrt{\sigma_1/\sigma_3}-\sqrt{\sigma_3/\sigma_1})/2)$. The relations between the macroscopic stress-strains and the microstructures on the mobilized plane obtained from the DEM simulation test at p=50 kPa are shown in Figure 10. It is seen that eqs. (2) and (3), which were originally obtained from simple and direct shear tests, are also applicable to biaxial shearing tests, further verifying that the macroscopic stress-strains (τ/σ_N, $-\mathrm{d}\varepsilon_N/\mathrm{d}\gamma$) are linearly well related to the microstructure quantities ($\overline{\phi_c}$, $\bar{\theta}$) on the mobilized plane.

$\overline{\phi_c}$ in eq. (2) can be expressed in the form[7,8]

$$\overline{\varphi_c}\cong\bar{\theta}+\frac{k}{f_0}\left(1.5\bar{\theta}^2+\frac{\pi^2}{24}\right)=\bar{\theta}+\delta, \tag{6}$$

in which $\bar{\theta}$ is the average particle contact angle, representing the particle geometric arrangement (fabric), f_0 the average contact force on the mobilized planes, k the gradient of a straight line that characterizes the distribution of the average particle contact forces on the mobilized planes. The ratio of k/f_0 represents the biased degree of the distribution of the particle contact forces to the positive zone of θ (along the shear direction). As the mobilized internal friction angle of granular materials is defined by $\phi_{\mathrm{mo}}=\tan^{-1}(\tau/\sigma_N)$, it is understood from eq. (6) that the mobilized internal friction angle is related to the granular fabric, the average contact force and its increasing degree along the shear direction, not directly related to the inter-particle friction as commonly recognized. Further investigation indicates that the second term of eq. (6), δ, can be regarded as a constant as it varies slightly during shearing. Thus, the particle contact angle θ representing particle fabric is closely related to the shear strength of granular materials.

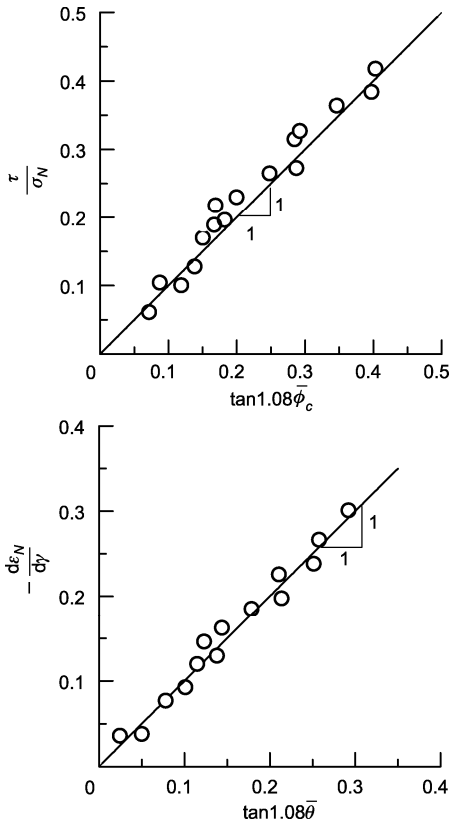

Figure 10 Relationships between the macroscopic stress-strains of granular materials with the microstructures on the mobilized plane.

4 Yield function of granular materials based on microstructures

Most of the yield functions of the existing elastic-plastic constitutive models for soils have been obtained macroscopically from laboratory triaxial compression tests.

For example, Cam-clay model[23,24] was based on the results of triaxial compression tests on normally consolidated clays, in which an experimentally obtained stress-dilatancy relationship was used and plastic volumetric strain is taken as hardening parameter; Tsinghua model[25] established its plastic potential function directly from the results of triaxial compression tests, and determined the hardening parameter on a hypothesis that yield surface is the same as plastic potential. As the yielding of granular materials is inevitably accompanied with the change of the microstructures of particles[26], and the distribution $N(\alpha)$ of particle contact points against contact angles α is a significant parameter to characterize the microstructures, it is thus possible to use $N(\alpha)$ as a hardening parameter to describe the yielding of granular materials.

As stated above, $N(\alpha)$ of granular materials changes during compression and shearing, namely, $N(\alpha)$ is directly affected by stress states. It is an internal variable that reflects the changing degree of granular material microstructures after the application of external stresses. Therefore, $N(\alpha)$ may be used as a hardening parameter to quantitatively describe the yielding of granular materials.

Here, we consider the change of $N(\alpha)$ along two stress paths: one is the isotropic compression path from a certain mean stress p, i.e. gradually increasing p; the other is the shearing path at a constant p, i.e. increasing σ_1 and decreasing σ_3 simultaneously so as to gradually increase the stress ratio σ_1/σ_3, as shown in Figure 11.

As discussed above, under isotropic compression, particle contact points are uniformly distributed with respect to contact angles. The distribution $N(\alpha)$ may be fitted using a circle, whose radius represents particle contact numbers in accordance with contact angle α. Thereafter, $N(\alpha)$ is briefly denoted as N. As mean stress increases from p to p_x, the circle's radius changes from N to N_x, whose increment $\Delta N_p=N_x-N$. During isotropic compression, the distribution increments ΔN_p of particle contact points obtained from DEM simulation are plotted against the increase of mean stresses $\Delta p=p_x-p$ in Figure 12. It is seen that the relationship between ΔN_p and Δp during isotropic compression can be fitted using an index equation no matter what initial mean stress p is. For the simulated sample, this index equation is expressed as follows:

$$\frac{\Delta N_p}{N}=0.009755\left(\frac{p_x-p}{p}\right)^{0.6}. \tag{7}$$

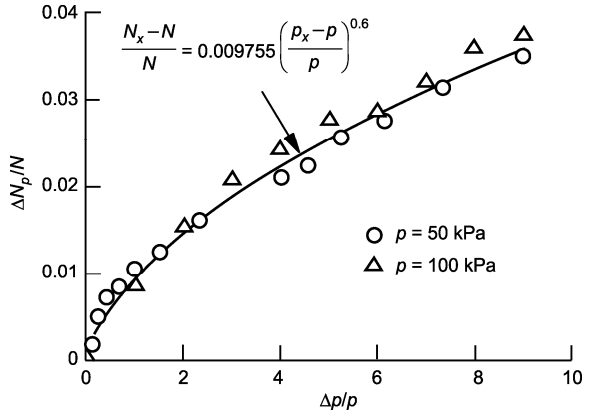

Figure 12 Distribution change of particle contact points during isotropic compression.

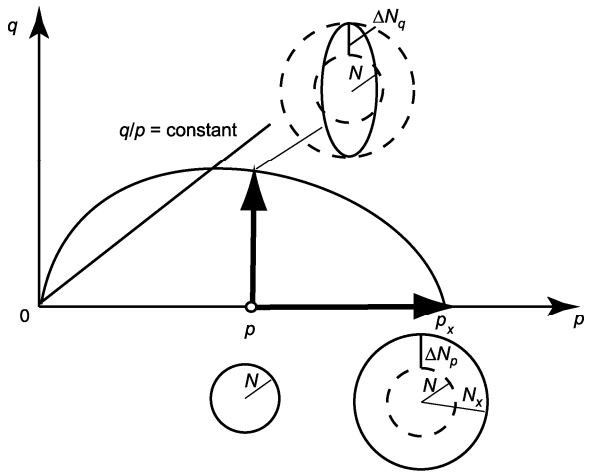

Figure 11 Schematic diagram of $N(\alpha)$ change under isotropic compression and during shearing at constant p.

Figure 13 indicates the numerically simulated distribution variation of particle contact points during shear processes under the condition of constant p. In Figure 13, ΔN_q is the sum of the increase of particle contact points along σ_1 and the decrease along σ_3, equivalent to the macroscopic deviator stress $q=\sigma_1-\sigma_3$. It is seen that during shearing, the distribution variation ΔN_q of particle contact points against the macroscopic deviator stress q may be fitted in a straight line. For the simulated sample, the straight line is expressed as

$$\Delta N_q/N=0.012(q/p). \tag{8}$$

It is assumed from a microscopic view that the distribution change ΔN_p during isotropic compression starting from a mean stress p is the same as the distribution change ΔN_q during shearing at the constant mean stress

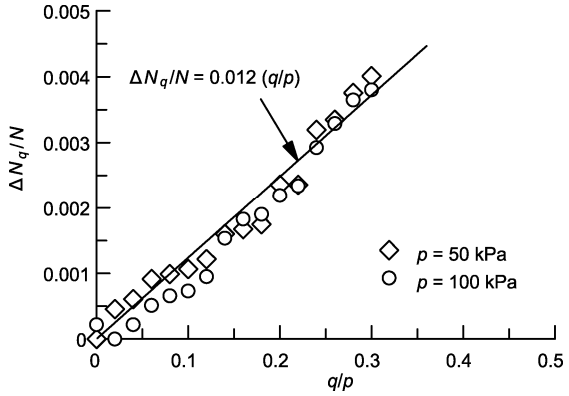

Figure 13 Distribution change of particle contact points during shearing at constant p.

p when a granular material yields (*cf.* Figure 11), that is

$$\Delta N_p = \Delta N_q. \tag{9}$$

Consequently, from eqs. (7), (8) and (9), we can obtain a yield function of granular materials based on the change of microstructures, which is expressed as

$$f = \frac{q}{p} - \kappa\left(\frac{p_x}{p} - 1\right)^n = 0, \tag{10}$$

where κ and n are the parameters reflecting the changes of granular structures. For the sample simulated in this article, κ=0.813, n=0.6. p_x is the mean stress where yield surface intersects with p-axial. The yield surface drawn from eq. (10) by taking κ=0.813 and n=0.6 is shown in Figure 14. In the same figure, for comparison, the yield surfaces of the original and modified Cam-clay models are also given, whose yielding functions are:

original Cam-clay model:

$$f = \frac{q}{p} - M \ln \frac{p_x}{p} = 0; \tag{11}$$

modified Cam-clay model:

$$f = q^2 + M^2(p^2 - p_x p) = 0. \tag{12}$$

In Figure 14, the parameter M used in Cam-clay models is taken as 0.856, which is calculated from

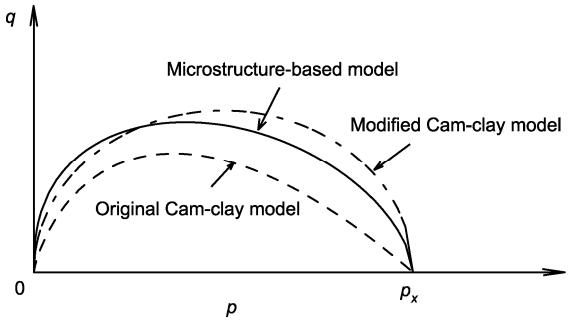

Figure 14 Yield surface of granular materials based on the distribution change of particle contact points.

$6\sin\phi/(3-\sin\phi)$ with ϕ=22° (*cf.* Figure 3). It is seen from Figure 14 that the shape of the yield surface based on the changes of granular microstructures is very similar to that of Cam-clay models, especially to that of the modified Cam-clay model. In Figure 14, the yield surface changes with the mean stress p_x. In Cam-clay models, p_x is related to the plastic volumetric strain, namely, the hardening parameter is the plastic volumetric strain. In fact, plastic volumetric strain is directly relevant to void ratio e, which represents the particles' geometric arrangement and reflects particles' microstructures. Thus, the hardening parameter of plastic volumetric strain in Cam-clay models indirectly reflects the changes of particle microstructures. In eq. (10), p_x is directly related to the distribution of particle contact points with respect to the contact angles, which is fitted with a circle. The radius of the distribution circle increases with the increasing p_x, reflecting the changes of particle microstructures. Therefore, it may be understood that the yield function of eq. (10) takes the distribution of particle contact points as its hardening parameter, which corresponds to the plastic volumetric strain as used in Cam-clay models. Therefore, the study on the yielding of granular materials based on their microstructures is helpful to understand the essence of granular materials.

5 Conclusions

In this work, a granular materials' biaxial compression test is numerically simulated by DEM. The changes of granular microstructures during isotropic compression and shear process are investigated, on which a yielding function is derived. The main results are as follows:

(1) The particle contact points are uniformly distributed with respect to the contact angles in a granular isotropically compressed media. The distribution reflects the particle microstructures and may be fitted with a circle. The circle's radius increases with the increasing mean stress p.

(2) During shearing, the shape of particle contact points' distribution gradually changes from a circle to an ellipse (or peanuts-like). This change is due to the appearing of particle contact points along σ_1 direction and the disappearing of particle contact points along σ_3 direction as well as the change of particle contact angles of steady contacts. The change of particle contact angles of steady contacts is controlled by the friction motion law between particles.

(3) During shearing, there exist good linear relations between the macroscopic stress-strains (τ/σ_N, $-\mathrm{d}\varepsilon_N/\mathrm{d}\gamma$) and the microstructure quantities ($\overline{\phi_c}$, $\overline{\theta}$) on the mobilized plane.

(4) The distribution of particle contact points with respect to the contact angles is a significant index of reflecting particles' microstructures. The derived yield function indicates the granular materials' yield characteristics during isotropic compression and shear processes via the distribution changes of particle contact points. Its shape is very similar to that of the modified Cam-clay model.

1 Oda M. Initial fabrics and their relations to mechanical properties of granular material. Soils Found, 1972, 12: 17－36
2 Matsuoka H. A microscopic study on shear mechanism of granular materials. Soils Found, 1974, 14: 29－43
3 Wang Y Y, Zhang Q D, Chen X Q, et al. Stress-strain self-organization Critical properties of debris flow (in Chinese). Chinese Sci Bull (Chinese Ver), 2003, 48: 976－980
4 Zhao C G, Zhang X D. Derivation of the work expression and discussion on the effective principle and the phase separation theorem in unsaturated soil. Sci China Ser E-Tech Sci, 2008, 51: 1530－1541
5 Zheng M S, Jin Z H. Spatially-cyclic function method of thermal stress analysis on grain intensified material (in Chinese). Chinese Sci Bull (Chinese Ver), 1994, 39: 1241－1245
6 Cundall P A, Strack O D L. A discrete numerical model for granular assemblies. Geotechnique, 1979, 29: 47－65
7 Liu S H, Matsuoka H. Microscopic interpretation on a stress-dilatancy relationship of granular materials. Soils Found, 2003, 43: 73－84
8 Liu S H. Simulating direct shear test by DEM. Canad Geotech J, 2006, 43: 155－168
9 Liu S H, Sun D A. Simulating the collapse of unsaturated soil by DEM. Int J Numer Anal Meth Geomech, 2002, 26: 633－646
10 Liu S H, Sun D A, Wang Y S. Numerical study of soil collapse behaviors by discrete element modeling. Comput Geotech, 2003, 30: 399－408
11 Chen H, Liu S H. Failure characteristics and stabilization methods. Canad Geotech J, 2007, 44: 377－391
12 Liu S H, Bauer E. A microscopic study of rainfall-induced granular slope failure. In: Proceedings of the 3rd Asian Conference on Unsaturated Soils, Nanjing, China, 2007. 379－383
13 Zhou J, Chi Y W, Chi Y, et al. Simulation of biaxial test on sand by particle flow code (in Chinese). Chinese J Geotech Eng, 2000, 22: 701－704
14 Liu Y, Wu S C, Zhou J. Numerical simulation of sand deformation under monotonic loading and mesomechanical analysis (in Chinese). Rock Soil Mech, 2008, 29: 3199－3207
15 Roak R J. Formulas for stress and strain. 4th ed. New York: McGraw-Hill, 1965. 319－321
16 Liu S H, Lu T H. Microscopic shear mechanism of granular materials in simple shear by DEM (in Chinese). Chinese J Geotech Eng, 2000, 22: 608－611
17 Liu S H, Xu Y F. Numerical simulation for a direct box shear test on granular marerial and microscopic consideration (in Chinese). Chinese J Rock Mech Eng, 2001, 20: 288－292
18 Satake M. Fabric tensor in granular materials. In: IUTAM Conference on Deformation and Flow of Granular Materials, 1982, 63－68
19 Xie D Y, Qi J L. Soil structure characteristics and new approach in research on its quantitative parameter (in Chinese). Chinese J Geotech Eng, 1999, 21: 651－656
20 Matsuoka H, Takeda K. A stress-strain relationship for granular materials derived from microscopic shear mechanism. Soils Found, 1980, 20: 45－58
21 Matsuoka H, Yamamoto S. A microscopic study on shear mechanism of granular materials by DEM (in Japanese). J Geotech Eng, 1994, 487/III-26: 167－175
22 Oda M, Konishi J, Nemat-Nasser S. Experimental micromechanical evaluation of granular materials: Effects of particle rolling. Mech Mater, 1982, 1: 269－283
23 Roscoe K H, Burland J B. On the generalized stress-strain behavior of 'wet' clay. In: Engineering Plasticity. Cambridge: Cambridge University Press, 1968. 535－609
24 Roscoe K H, Schofield A N, Thurairajah A. Yielding of clay in states wetter than critical. Geotechnique, 1963, 13: 221－240
25 Huang W X, Pu J L, Chen Y J. Hardening rule and yield function for soil. In: Proceedings of the 10th International Conference on Soil Mechanics and Foundations Engineering, 1981. 631－634
26 Matsuoka H, Akashi Y, Itoh K, et al. Deformation of yield surface based on fabric of granular material and its experimental check. In: Proceedings of the 30th Japan National Conference on Soil Mechanics and Foundations Engineering, 1995. 579－582